Design of Compensator to Regulate Multivariable Coupled System

Jaya Prakasa Rao ch¹, N. D. Sridhar², Ramalla Issac³

¹Research Scholar, Department of Electrical Engineering, Annamalai University, Annamalai Nagar – 608002, Tamil Nadu,India.; peprakash@gmail.com

²Department of Electrical and Electronics Engineering, Annamalai University, Annamalainagar – 608002, Tamil Nadu, India; sridarnd1@gmail.com

³Department of Electrical and Electronics Engineering, Marri Laxman Reddy Institute of Technology and Management Dundigal, Hyderabad – 500 043, Telangana, India; issac@gmail.com

The primary objective of this work is to select the sliding mode transition function in order to regulate the multivariable coupled system. An inverter working as a parallel active power filter with three phases and three wires is controlled using a sliding mode control technique. There is no need to split the system model created in the "dq" synchronous reference frame into two different rounds. Furthermore, higher stability and resilience across a broad operating range are made possible by the suggested control method. Variable switching properties are seen when pulse switches are controlled by sinusoidal pulses. For continuous switching of the converter switches, spatial vector modulation provides the active filter pulses. However, if used in practice, standard spatial vector modulation calls for a complicated method that uses trigonometric functions like arctan, sine, and cosine, which in turn calls for lookup tables to store the previously calculated trigonometric values. Using only the inverter voltage and current sensed in this study, a substantially simplified approach is provided to create spatial vector modulation pulses for six switches. An active shunt filter is created by the voltage source. Very good findings are verified through simulation using PSIM and MATLAB tools. The findings demonstrate that the controller's suggested positioning and optimal gain settings successfully reduce the LFO. Additionally, it improves system stability and transient capacity in the presence of severe turbulence.

Keywords: Thyristor Controller Series Compensator (TCSC), Dynamic Stability, Variable Structure Control, eigen values, Damping Ratio.

1. Introduction

Currently, EPS is being used extensively due to increased demand for electricity from existing transmission lines and a shortage of new transmission lines. [beginning]. In the presence of small disturbances, dynamic instability generates oscillations with increasing amplitude in the range of 0.2 to 2.0 Hz. Without proper damping stabilizers, the system becomes unstable [2].

To reduce oscillations, place a power stabilizer (PSS) on the exciter. Under heavy loads, PSS cannot provide sufficient damping results because the system becomes unstable [3]. To overcome the limitations of PSS, we used FACTS series controllers such as TCSC to improve dynamic stability. FACTS controllers are more economical than new transmission systems [4].

The linearized model of the PI controller ensures optimal performance at the operating point. However, when the operating points and system parameters are different, the damping controller's fixed structure does not provide optimal performance.

Variations in system parameters are compensated by an adaptive controller [5]. System performance is improved thanks to an adaptive controller that changes system parameters. However, adaptive controllers require online observation of network states to determine system parameters and to quickly calculate state feedback gains. This method is limited to simple low-order systems, so performance is not optimal.

An intelligent controller has been implemented to reduce the LFO. Fuzzy logic controllers, Fuzzy PID and FOPID are intelligent controllers. These controllers are not suitable for parameter variations or sudden load disturbances. This is the main limitation of this controller [6, 7].

To overcome the above limitations, alternative control strategies have been proposed. To overcome the above limitations and improve the stability of the network, a modern nonlinear feedback controller is proposed. When sudden disturbances occur in the system, the VSC controller becomes more sensitive to parameter changes. In this article, we propose a nonlinear controller such as a slider as a control strategy. When sudden load disturbances or parameter changes occur, the mathematical models of these controllers are adjusted to improve the dynamic stability of the system [8].

Outkin et al. [9] proposed three alternative methods to select the resulting switching vector. Sliding motion has desirable properties. In the first model of the system, the sliding motion is represented by a mathematical equation with equally spaced eigenvalues. The second problem involves minimizing the square of its value with respect to the state vector, and the third problem involves minimizing the sliding-equivalent control problem that controls the cost in sliding mode. The third is to minimize performance indicators and corresponding control issues related to controlling rolling operating costs.

Therefore,mentioned literature review shows that conventional controllers do not provide sufficient damping and require more time to reach the steady state point when sudden disturbances occur. To overcome this difficulty, a nonlinear feedback controller is proposed, namely H. VSC based on sliding mode. The stability of the network depends on the sliding surface control law. The control law forces the trajectory of states to change infinitely to *Nanotechnology Perceptions* Vol. 20 No.6 (2024)

achieve the control goal. Modified structure with line stabilizer applies VSC theory to single-machine systems and improves system damping in critical modes at rated load compared to conventional controllers. Systematic description of the critical mode switching hyperplane and the switching vector for the two state variables $\Delta\delta$ and $\Delta\omega$ [10]. Its VSPSS recommendation, ideal for multi-machine networks. The proposed method is optimized by selecting the switching hyperplane according to the squared power index to minimize the running time in sliding mode. The optimal selection of the weight matrix in the performance metrics for converting between hyperplane and vector is very difficult [11,12]

A variable output feedback structure was applied to a single machine infinite bus (SMIB) system using TCSC. The input signal of the

VSC is considered as active power and reactive power. The effectiveness of the controller is demonstrated through time domain analysis. VSC provides superior dynamic performance in critical modes of the test system compared to TCSC feedback and no TCSC [13].

The mathematical analysis, current insertion design, and dynamic modelling of the first suggested FACTS device in the series are the study's key goals. H. VSC and TCSC. To increase the network's damping ratio (DR), a variable output feedback gain control is suggested in this work. It would move the critical mode to the left side of the S-plane. Speed is employed as the response variable, as opposed to the study by [14]. Additionally, VSC is unaffected by changes in parameter values. To gradually increase muscle input power, the performance of the variable TCSC construct was compared to the TCSC response with PSS and without control.

A computer simulation is run on an EPS with TCSC to show the viability of the suggested output response VSC. The simulation findings demonstrate that the suggested variable structure with TCSC can enhance the network's damping properties when compared to a single system's TCSC response at rated load with PSS. Can anything be drawn from this?

2. System investigated

As illustrated in Figure 1, we looked into the SMIB system's small-signal model to assess the local LFO. For a private system, the IEEE Type 1 exciter and flux decay model of this machine was taken into consideration [15]. The linearized Heffron-Phillips (HP) model underwent dynamic stability investigation is depicted in Figure 2. Reference [16] contains data on dynamics and excitation.

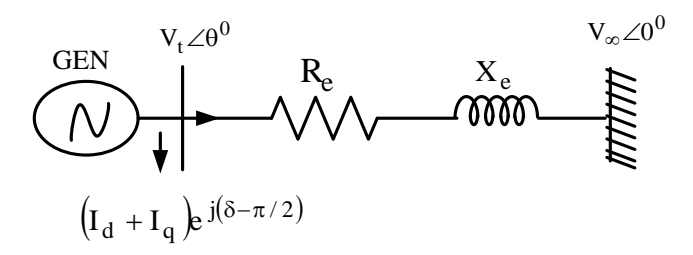


Fig.1:Schematic diagram of a SMIB bus system.

The starting values of various variables are calculated using steady state equations in order to determine the K constant. The K constant is disabled in Figure 2. K_1 to K_6 as 0.78, 0.63, 0.39, 0.975,0.038 and 0.698.

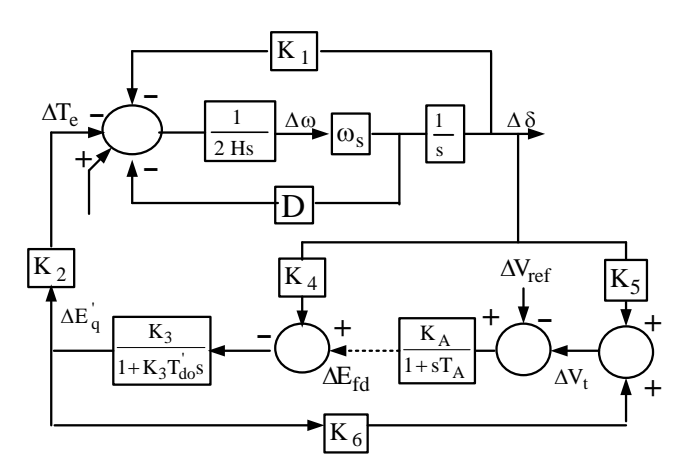


Fig.2. Linearized HP model for a SMIB system.

The Differential Algebraic Equation (DAE) of the EPS is expressed as follows [15]

$$\dot{X} = f(X, Y) \qquad (1)$$

$$0 = g(X, Y) \qquad (2)$$

Equation (1) in Figure 1 represents the differential equation for the generator and load, whereas Equation (2) represents the algebraic equation. To derive the eigenvalues from the system matrix, linearize the given equation.

$$\dot{X} = AX + BU$$

$$Y = CX$$
(4)

Where 'U' stands for the control/input vector, 'X' stands for the state vector, and 'Y' is the output vector. The state matrix is represented by matrix A, the control matrix by matrix B, and the output matrix by matrix C.

Where,

$$X = \begin{pmatrix} \Delta E_q{'} & \Delta \delta \Delta \omega & \Delta E_{fd} \end{pmatrix} \text{ and } u = \begin{bmatrix} \Delta T_M & \Delta V_{ref} \end{bmatrix}$$

The system matrix'A' is the order of 4×4

$$A = \begin{bmatrix} -0.4304 & -0.1654 & 0 & 0.1695 \\ 0 & 0 & 314 & 0 \\ -0.1000 & -0.2000 & 0 & 0 \\ -1.3997e + 003 & -76.9468 & 0 & -5 \end{bmatrix}$$

The matrix'B' is the order of 4×2

$$\mathbf{B} = \begin{bmatrix} 0 & 0 \\ 0 & 0 \\ 0.2110 & 0 \\ 0 & 2000 \end{bmatrix}$$

The matrix'C' is the order of 1×4

$$C = \begin{bmatrix} 0 & 0 & 1 & 0 \end{bmatrix}$$

and also, without controller the transfer function of the system is

$$\frac{0.211s^3 + 1.146 s^2 + 50.43 s + 1.091 e - 011}{s^4 + 5.43 s^3 + 291.3 s^2 + 276.8 s + 11910}$$

There are 4 eigenvalues for the transfer function mentioned above. Determine the A-matrix's eigenvalues using Equation (3). The test system's eigenvalues without a damping controller are shown in Table 1.

Mode#	Withoutcontrol	DR(ζ)	Frequency (rad/sec)
$\Lambda_{1,2}$	-2.5872 ± 14.3260 i	0.1738	15.62
$\Lambda_{3,4}$	-0.0245 ± 7.1202i	0.00342	7.78

Table.1. Eigenvalues of the SMIB system.

The critical mode has a modest $\Lambda_{3,4}$ and low DR of 0.00342, which is why it is called that. Table. 1 Because of the critical mode's low damping, oscillations grow exponentially and never reach a stable state. To improve the dynamic stability of the network, the damping controllers PSS and TCSC are mounted to the machine.

3. PSS

By adding supplemental damping to the rotor excitation, PSS eliminates the negative damping. Three blocks are seen in Fig. 3. The critical mode's $\Lambda_{3,4}$ damping is produced by the gain block. The block 2 is omitted and in block 3, The damping torque for the modes is produced by the time constants T_1 and T_2 .

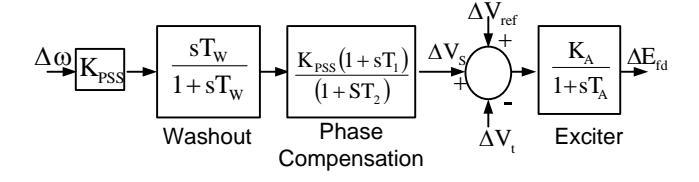


Fig.3. IEEE Type-1 exciter with PSS

The Deviation of speed from synchronous speed i.e $\Delta \omega_m$, and deviation of voltage i.e ΔV_S , are the input and output of PSS damping controller. At the summing point ΔV_S is combined Nanotechnology Perceptions Vol. 20 No.6 (2024)

with ΔV_{ref} and ΔV_t , so as to mitigate the oscillations in the network [2,14]. The calculation of system matrix (A_{SYS}), B and C equations of the system with PSS are presented in [16].

The input to the PSS is $\Delta \omega_m$, and ΔV_S is the output of the PSS. To mitigate the oscillations, at the summing point ΔV_S , ΔV_t and ΔV_{ref} are combine [2]. After, the insertion of PSS, the system matrix A_{SVS} , B and C equations are presented in [16].

Mode ≠	System with PSS	DR (ζ)	Frequency
			(rad/sec)
$\Lambda_{1,2}$	-2.2125 ± 15.48i	0.1825	15.6
$\Lambda_{3,4}$	$-0.3792 \pm 7.755i$	0.0501	7.57
$\Lambda_{5,6}$	-10.4290	1.0	10.40

Table.2. Eigenvalues of thenetwork with PSS.

The DR of the crucial mode in Table 2 is enhanced from 0.00342 to 0.0501 with the addition of PSS. The DR of the mode gets better, but by connecting the TCSC to the network, it can get even better.

4. TCSC

As indicated in Fig. 1, the system being studied consists of a synchronous generator connected to a large power system via a transmission line with a TCSC. A TCSC controller manages the variable series compensation, Dx, that the TCSC offers. The next section will construct a variable structure TCSC controller to enhance the dampening of system oscillations. The block diagram of the excitation system is shown in Fig. 2, and it may be characterized by the differential equations shown below[17].

The transmission line is connected in series with the TCSC controller. The series reactance in the transmission line changes as the firing angle changes. The TCSC damping controller is shown in Fig. 4.

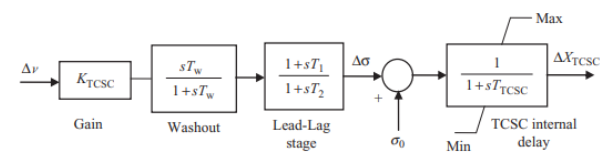


Fig.4.TCSC damping controller.

In Fig. 4, there are three blocks that resemble PSS damping controllers [13]. By varying the firing angle, the system's net reactance will change, which improves the damping of the system. When TCSC is added, the two state variables, $\Delta \propto$ and ΔX_{TCSC} are added to the generator state matrix of Equ. (3). Results the eigenvalues of the system matrix increased by two. The values of TCSC are presented in [15].

The K - constants for SMIB system with TCSC are calculated using the equations given in [16].

$$K_3 = 0.5313$$
, $K_4 = 0.4952$, $K_1 = 0.9751$, $K_2 = 0.5668$,

$$K_5 = 0.0374$$
, and $K_6 = 0.8231$

$$\mathbf{X} = \begin{bmatrix} \Delta \mathbf{E_q}' & \Delta \boldsymbol{\delta} & \Delta \omega \Delta \mathbf{E_{fd}} & \Delta \propto & \Delta \mathbf{X_{TCSC}} \end{bmatrix}$$
 (5)
$$\mathbf{A_TCSC} = \begin{bmatrix} -0.302 & -0.1 & 0 & 0.5 & 0 & 0 \\ 0 & 0 & 314 & 0 & 1 & 0 \\ -0.1 & -0.21 & 0 & 0 & 0.62 & 0 \\ -1653.3 & -75.7 & 0 & -5.0 & 2003 & 0 \\ 1.520 & 2.65 & -43 & 0 & -20.8 & 0 \\ 0 & 0 & 0 & 0 & 0 & 0 \end{bmatrix}$$

$$B_TCSC = \begin{bmatrix} 0 & 0 \\ 0 & 0 \\ 0.22 & 0 \\ 0 & 2005 \\ -4.35 & 0 \\ 0 & 0 \end{bmatrix}$$

$$C_{TCSC} = \begin{bmatrix} 0 & 0 & 3 & 0 & 0 & 0 \end{bmatrix}$$

and also, the transfer function of the system with TCSC controller is

$$\frac{0.212 s^5 + 3.34 s^4 + 71.58 s^3 + 567.9 s + 25.78 s}{s^6 + 27.18 s^5 + 463.2 s^4 + 6075 s^3 + 18270 s^2 + 11780 s + 4287}$$

For the above transfer function, 6 eigenvalues are present. Table. 3, represents the eigenvalues of the test system after insertion of TCSC. The critical mode DR improved to 0.2050 from 0.0501, respectively.

Mode ≠	System with TCSC	DR (ζ)	Frequency
			(rad/sec)
$\Lambda_{1,2}$	-3.2100 ± 16.10 i	0.1960	16.400
$\Lambda_{3,4}$	-0.9710 ± 4.63 i	0.2050	4.73
$\Lambda_{5,6}$	-0.040,-17.80	1.0, 1.0	0.040, 17.80

Table 3. Eigenvalues of test system with feedback TCSCdamping controller.

5. Variable Structure System (VSS)

To enhance the dynamic stability, the damping effect significantly improved by the control signal ${}'\mathbf{u}'$, from the Eq. 3. For different operating points, the damping effect can be significantly improved.

The state feedback for the linear state regulator is designed as

$$\mathbf{U} = \mathbf{K}^{\mathsf{T}}.\mathbf{X} \tag{6}$$

K is the feedback gain matrix in Equation (6) above, and it is chosen using the quadratic minimization strategy.

A change in structure occurs at the switching hyperplane and is known as the switching function.

$$\mathbf{S} = \mathbf{G}^{\mathsf{T}} \mathbf{X} = \mathbf{0} \quad (7)$$

In equ. (7), '**G**', represents the constant vector.

The following are the requirements for sliding modes states to occur on a sliding surface:

$$Lt_{S\to 0}$$
- $\dot{S}>0$ and $Lt_{S\to 0}$ + $\dot{S}<0$

The aforementioned conditions are necessary for sliding mode to exist

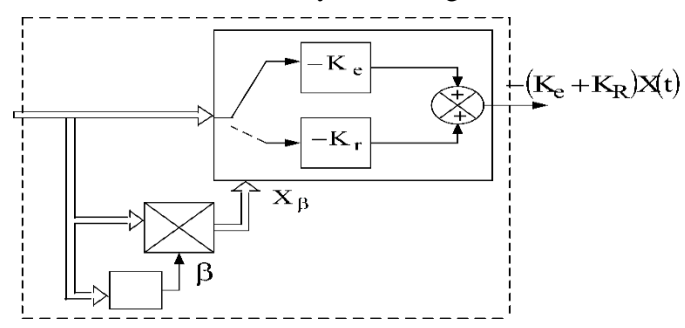


Fig.5. Block diagram representation of Variable Structure with TCSC.

The block diagram of VSS is depicted in Fig. 5. There are two steps in this Fig. 5. The control rule (K_e) , which places the state trajectories on the sliding surface (S), is the first stage. The second stage (K_r) , which moves the states to the sliding surface, is the third stage [18-20].

Creating Variable Structures Power system thyristor-controlled series compensator with desired eigenvalues operating in sliding mode

TCSC is used in series with a transmission line to improve the dynamic stability. The TCSC may adjust its apparent reactance smoothly and quickly by altering the thyristors' firing angles [21].

The first (n-1) rows of the transformation matrix M are chosen to be orthogonal to vector b, and the product of the nth row of M and b is chosen to be non-zero. M is therefore chosen as

$$\mathbf{M} = \begin{bmatrix} 1 & 0 & 0 & 0 & 0 & 0 \\ 0 & 1 & 0 & 0 & 0 & 0 \\ 0 & 0 & 1 & 0 & 0 & 0 \\ 0 & 0 & 0 & 1 & 0 & 0 \\ 0 & 0 & 0 & 0 & 0 & 1 \\ 0 & 0 & 0 & 0 & 1 & 0 \\ \end{bmatrix}$$

The order of 'M' is 6×6

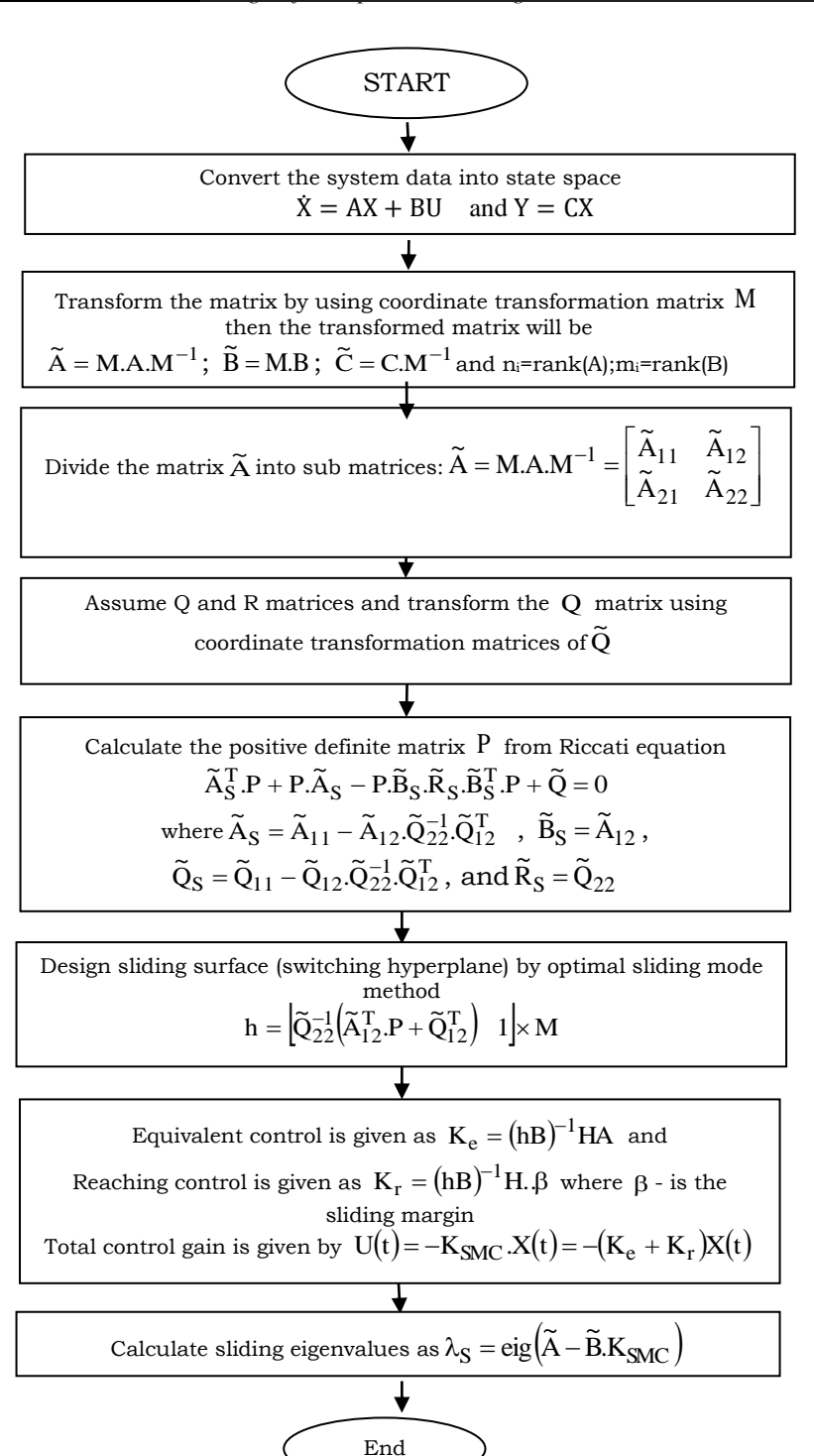


Figure 6. Flowchart for a test system's variable structure controller and TCSC

Apply the coordinate transformation, $\mathbf{Z} = \mathbf{M}\mathbf{X}$, the matrices A_{11}, A_{12}, A_{21} and A_{22} of the matrix $MA_{SVeC}M^{-1}$ for the system investigated, are:

 \tilde{A} is the order of 6×6

 $\tilde{A}_{11} = (n_i - m_i) \times (n_i - m_i)$ and it is the order of 4×4

$$\widetilde{A}_{11} = \begin{bmatrix} -0.3 & -0.1 & 0 & 0.2 \\ 0 & 0 & 314 & 0 \\ -0.1 & -0.1 & 0 & 0 \\ -1646 & -74.7 & 0 & -5 \end{bmatrix}$$

 $\widetilde{A}_{12} = (n_i - m_i) \times m_i$ and it is the order of 4×2

$$\widetilde{\mathbf{A}}_{12} = \begin{bmatrix} 0 & 0 \\ 0 & 0 \\ 0 & 0.5 \\ 0 & 2000 \end{bmatrix}$$

 $\tilde{A}_{21} = m_i \times (n_i - m_i)$ and it is the order of 2×4

$$\widetilde{A}_{21} = \begin{bmatrix} 0 & 0 & 0 & 0 \\ 1.5 & 2.5 & -40 & 0 \end{bmatrix}$$

 $\tilde{A}_{22} = m_i \times m_i$ and it is the order of 2×2

$$\widetilde{A}_{22} = \begin{bmatrix} 0 & 0 \\ 0 & -20.8 \end{bmatrix}$$

CALCULATE 'P' MATRIX: P is the solution of Riccati equation

$$\widetilde{P}_{SMC} = \begin{bmatrix} 41.8 & -8.5 & 136.7 & -0.0 \\ -8.5 & 2.4 & 2.5 & -0.0 \\ 136.7 & 2.5 & 9730.7 & -2.4 \\ -0.00 & -0.0 & -2.4 & 0.0 \end{bmatrix} \widetilde{S}_{SMC} \begin{bmatrix} -1999.8 \\ -0.4 + i5.1 \\ -0.4 - i5.1 \\ -1.0 \end{bmatrix}$$

$$\widetilde{K}_{SMC} = \begin{bmatrix} 0 & 0 & 0 & 0 \\ 7.0376 & -1.5559 & 39.4342 & 0.9883 \end{bmatrix}$$

Sliding surface S or h:

This switching sliding surface is a function of portioned $\widetilde{A},\widetilde{Q}$ matrices and transformed matrix (M).

$$S = \left[\widetilde{Q}_{22}^{-1}\left(\widetilde{A}_{12}^{'}.P_{SMC} + \widetilde{Q}_{12}^{'}\right) \quad I\right] * M$$

$$\mathbf{h}_{SMC} = \begin{bmatrix} 0 & 0 & 0 & 0 & 1.0 & 1.0 \\ 7.0376 & -1.5559 & 39.4342 & 0.9883 & 1.00 & 1.0 \end{bmatrix}$$

$$K_{eSMC} = (H_{SMC}.\tilde{B})^{-1}.H.\tilde{A}$$

$$K_{eSMC} = \begin{bmatrix} -0.3437 & -0.5912 & 9.4800 & 0 & 0.0095 & 4.9447 \\ -0.8213 & -0.0377 & -0.2871 & -0.0019 & -0.00 & 0.9900 \end{bmatrix}$$

 K_{rSMC} = $\left(\!H_{SMC}.\widetilde{B}\right)^{\!-1}\!.H.\delta$, where $\,\delta$ is the sliding margin and it is assumed to be 0.85

$$\begin{split} K_{rSMC} = & \left(H_{SMC}.B \right) \ .H.8 \ , \text{ where } \delta \text{ is the sliding margin and it is assumed to be } 0.85 \\ K_{r} = & \begin{bmatrix} 0 & 0 & 0 & 0 & -0.2133 & -0.2133 \\ 0.0032 & -0.0007 & 0.0180 & 0.0005 & 0.0009 & 0.0009 \end{bmatrix}_{\ Linear \ feedback \ control \ law \ for \ VSS \ is \ given \ by \end{split}$$

VSS is given by

$$u = -KX = -(K_e + K_r)X = -(K_{eSMC} + K_{rSMC})x =$$

$$K_{SMC} = (K_{eSMC} + K_{rSMC})$$

$$K_{SMC} = (R_{eSMC} + R_{rSMC})$$

$$K_{SMC} = \begin{bmatrix} 0.3437 & 0.5912 & -9.4800 & 0 & 0.2038 & -4.7314 \\ 0.8211 & 0.0384 & 0.2691 & 0.0014 & -0.0009 & -0.9909 \end{bmatrix}$$
The dynamics of system states with

VSS is calculated from sliding eigenvalues

 λ_{S} (Sliding eigenvalues) = eig $(\tilde{A} - \tilde{B}.K_{SMC})$

Mode #	Sliding eigenvalues	$DR(\zeta)$	Frequency (rad/sec)
$\Lambda_{1,2}$	-4.8015 ± 22.376 i	0.2105	22.900
$\Lambda_{3,4}$	-1.3242 ± 4.6567 i	0.274	4.84
$\Lambda_{5,6}$	-34.7485, -0.0400	1,1	34.7485, 0.0400

Table.4. Eigenvalues of the SMIB system with Variable Structure TCSC

The eigenvalues of the network with variable structure TCSC are shown in Table.4. Since the system matrix has a 6th order, there are a total of 6 -eigenvalues, all of which are present on the left side of the s-plane and the network is dynamically stable. The DR is increased to 0.274 from 0.2050 as a result of the critical mode's eigenvalue (-1.3242+ 4.6567 i) being more moved to the imaginary axis of the s-plane. As a result, the system is more dynamically stable when in sliding mode than when it is not.

6. Results and Discussions

The suggested variable structure controller with TCSC is put to the test by subjecting the system to a step increase in mechanical input power, when running at nominal point P = 1.0p.u , Q = 0.67 p.u and $V_t=1.0$ p.u , the dynamic response of the system is presented in Fig.7[15,21].

This section's findings were produced with MATLAB. Figure 7 compares the dynamic stability of the test systems with and without damping control, with PSS, with feedback TCSC, and with variable structure with TCSC. The tests are run for 10 seconds to assess the system's performance.whereas ' $\Delta\delta$ ' is the rotor angle of machine synchronous machine, respectively.

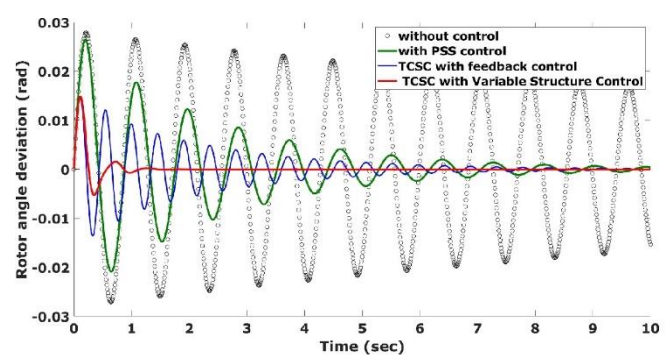


Fig.7. Rotor angle deviation $\Delta \delta$ '(rad) of the SMIBsystem without control (black line with circles), with PSS (green colour line), with TCSC (blue colour line) and TCSC with variable structure (red colour line).

Without damping controllers, the system is unstable. This is because the electromechanical mode's eigenvalue, shown in Table 1 as -0.0242 ± 7.0200 i, has weak damping. PSS was attached to the exciter of the special system, and the bad damping critical eigenvalue changed from -0.0242 + 7.0200 i to -0.3792 ± 7.755 i (Table-2). The network's damping has increased to 0.0467, and the TCSC feedback control has further improved the damping.

Poor damping caused the TCSC's eigenvalue to move from -0.3792 ± 7.755 i to -0.9710 ± 4.63 i (Table 3). The mechanism now has better damping. In fact, compared to using PSS or a controller-less oscillation, the oscillation mode has stabilized, and the selling time and peak overshoot have both been reduced. The system's oscillation mode with TCSC has been stabilized.

The critical eigenvalue is moved from $0.9710\pm4.63i$ (Table-3) to $-1.3242\pm4.6567i$ (Table-4) when comparing the variable structure controller with SVeC as feedback controller. As a result of improved system damping, the system is more stable. From the dynamic response curves, it can be shown that the variable structure TCSC stabilizes the system more than the TCSC feedback controller.

In Fig. 7,the settling time(t_s), of these oscillations for ' $\Delta\delta$ 'is t_s = 123.2857 s, 10.85 s, 4.385 s and 3.8771 s, and for peak overshoot (%M_P), the corresponding values are: without control, with PSS, with feedback TCSC, and with variable structure-based TCSC, respectively, 1.0095%, 0.8523, 0.4563%, and 0.2683%.

According to Fig. 7, the system with VSC has the smallest amplitudes, a shorter recovery time to pre-disturbance conditions, less settling time, less overshoot, and less undershoot.

The primary benefit of this controller is that the nonlinearities of the system are taken into account in sliding mode. The main drawback of this controller is that it is extremely

challenging for higher order systems. Because an observer-based sliding mode controller can avoid both the problem of system variables being unavailable and the difficulty in measuring system states

7. Conclusion

A structure for output feedback variables The TCSC controller was created to enhance a power system's dynamic performance. The suggested variable structure controller's utilization of only physically measurably speed deviation signals as controller inputs is one of its key features. This makes it reasonably simple to construct the suggested variable structure controller in practice. Additionally, while the system is run in sliding mode, the dynamic performance is relatively unaffected by changes in the operating circumstances and plant parameters. According to the results of the simulation, the variable structure TCSC controller offers a practical way to enhance the power system's damping characteristic.

References

- Anderson, P.M. Fouad, A.A (2003) Power System Control and Stability. John Wiley & Sons, India.
- Kundur, P, Balu, N J and Lauby M G (1994) Power system stability and control. McGraw-hill, New York.
- 3. Amin Safari, Hossein Shayeghi, Heidar Ali Shayanfar (2016) Coordinated control of pulse width modulation-based AC link series compensator and power system stabilizers. Electrical Power and Energy systems, 83: 117-123. https://doi.org/10.1016/j.ijepes.2016.03.042
- 4. Hingorani, N H, and Gyugyi. L(2000) Understanding FACTS: Concepts and Technology of Flexible AC Transmission System. Wiley- IEEE press, India
- 5. A. Ghosh, G Ledwich, O.P.Malik and G.S.Hope, (1984) Power System Stabilizer based on adaptive control techniques: IEEE Transactions on power Apparatus and Systems, 103: 1983-1989, DOI: 10.1109/TPAS.1984.318503
- 6. H. Shayeghi, H.A. Shayanfar., and Jalli (2009) Load Frequency Control Strategies: A state of the art Survey for the Researcher: Energy Conversion and Management. 50:344-353. https://doi.org/10.1016/j.enconman.2008.09.014
- 7. Ibraheem, Prabhat Kumar and DwarakaP.Kothari (2005) Recent Philosphies of Automatic Generation ControlStartegies in Power System. IEEE Transactions on Power Systems. 20:346-357. DOI: 10.1109/TPWRS.2004.840438
- 8. M.L. Kothari, J. Nanda, and K. Bhattacharya (1993) Design of variable structure power system stabilisers with desired eigenvalues in the sliding mode. IEE proceedings Generation, transmission and distribution 140:263-267. DOI:10.1049/ip-c.1993.0039
- 9. Utkin.I, and Yang,K.D (1978) Methods for constructing discontinuity planes in multidimensional variable structure systems:Automation and Remote control, 39: 1466-1470. DOI: 10.1016/0005-1098(78)90071-7
- 10. G. Venkataramanan and B.K. Johnson, (2002) Pulse width modulated series compensator," IEEE Proc. Gen. Trans and Dist, 149: 71-75, DOI:10.1049/ip-gtd:20020004.
- 11. CHAN, W.C., and HSU, Y.Y (1983) An optimal variable structure stabilizer for power system stabilization: IEEE Trans. Power apparatus and systems, 102: 1738-1746. DOI: 10.1109/TPAS.1983.317916
- 12. M.L. Kothari and CHAN (1983) Stabilization of power systems using a variable structure stabilizer. Electric Power Systems Research 6:129-139.

- 13. Tain-SyhLuor, Yuan-Yih Hsu (1998) Design of an output feedback variable structure thyristor-controlled series compensator for improving power system stability: Electrical Power Systems Research, 47: 71-77.https://doi.org/10.1016/S0378-7796(98)00049-2
- 14. G. Venkataraman an and B.K. Johnson, (2002) Pulse width modulated series compensator," IEEE Proc. Gen. Trans and Dist, 149: 71-75, DOI:10.1049/ip-gtd:20020004
- 15. Debasish Mondal, Abhijit Chakrabarti and Aparajita Sengupta(2014) Power System Small Signal Stability and Control. Academic Press, Elsevier, India.
- 16. K Himaja, T.S Surendra and S. Tara Kalyani (2021) Dynamic Stability Analysis of a SMIB system with PSS and LQR optimal control: Proc. ICIPTM, Noida, India. DOI: 10.1109/ICIPTM52218.2021.9388318.
- 17. Y. Welhazi, TawfikGuesmi, I. B. Jaoued and Hsan Haj Abdallah, "Power system stability enhancementusing FACTS controllers in multimachine power systems", Journal of Electrical Systems, vol. 10, no. 3, pp. 276-291, 2014.
- 18. Kai Liao, Zhengyou He, Yan Xu, Guo Chen, Zhao Yang Dong and Kit Po Wong (2017)A sliding mode based damping control of DFIG for interarea power oscillations:IEEE Transactions on sustainable Energy,8:258-267,DOI: 10.1109/TSTE.2016.2597306.
- 19. Lionel Leory Sonfack, Godpromesse Kenne and Andrew Muluh Fombu (2018) A new Static Synchronous Series Compensator control strategy based on SMIB system RBF Neuro-Sliding Mode technique for power flow control and DC voltage regulation: Electric Power Components and Systems, 46: 456-471, https://doi.org/10.1080/15325008.2018.1445795
- 20. F.L. Lewis, D. Vrable and V. L. Syrmos "Optimal control", (book) John Wiley. 1986.
- 21. M. Athans and P. Falb, "Optimal control: an introduction to the theory and its Application" (book) McGraw-Hill, 1966.